

# DETECTING DAMAGED ZONES ALONG SMART SELF-SENSORY CARBON BASED TRC BY TDR

GABEN MAHDI AND GOLDFELD YISKA\*

Faculty of Civil and Environmental Engineering, Technion – Israel Institute of Technology, Haifa, 32000, Israel

## ABSTRACT

The study aims to investigate the ability of smart self-sensory carbon roving to detect damaged zones in TRC structures. State of the art monitoring procedures are based on integrative measurements and accordingly are limited in detecting only the occurrence of damage. This study aims to handle this limitation and offers to adopt the Time Domain Reflectometer (TDR) technique. The TDR concept is widely used in Bayonet Nut Coupling (BNC) cables to identify defects along the cable (opens, shorts, etc.). The current study adopts its principle to carbon rovings. To simulate the BNC cable configuration, the study offers to connect two parallel carbon rovings to the TDR Data Acquisition (DAQ) system. The proposed monitoring technique is investigated by loading two textile reinforced MPC beams under uniaxial tensile loading. Results show the potential of the suggested technique to locate damage zones in TRC structures and highlights its limitation.

## KEYWORDS

Time domain reflectometer; Smart carbon rovings; AC measurements; Crack identification technique.

---

\* Corresponding author: Goldfeld Y., e-mail: [yiska@technion.ac.il](mailto:yiska@technion.ac.il)

## INTRODUCTION

Intelligent concrete structures with self-sensory capabilities are increasingly relevant in today's-built environment. The technology of carbon-based textile reinforced concrete (TRC) is a potential candidate for the development of such intelligent structures. Textile reinforcement technology is based on a biaxial textile mesh of alkali-resistant glass (AR-glass), carbon or basalt rovings with a high tensile strength and high resistance to corrosion. It allows to construct thin-walled, light and durable concrete elements [2,10,14]. Since the carbon rovings are electrically conductive, they can be used both as the main reinforcement system and as the sensory agent [1,4,5,13,16,17]. The potential of using carbon rovings as an integrated sensory agent has been presented in the literature for various sensory purposes such as: detecting cracking [7], estimating strain [7,13,16,17], monitoring the mechanical loading [1,4,5], identifying infiltration of water through cracked zones [6,12], etc. The commonly used approaches for the electrical measurement are based on direct current (DC) electrical circuits by two-probes monitoring setup [13], four-probes monitoring setup [16], Wheatstone bridge configurations [7,17], or by alternating current (AC) electrical circuits [4,5]. These studies proved the feasibility of the smart sensory concept and focused on the correlation between measured changes in the

electrical resistance (ERC), the electrical inductance or the electrical impedance of the carbon roving and the structural response. All the above-mentioned monitoring systems yield integrative measurements quantities that cannot localize damage along the structure. This study aims to detect the damaged zones by adopting the principles of the Time Domain Reflectometer (TDR) technique to smart carbon based TRC structures.

The principle of TDR is traditionally used in Bayonet Nut Coupling (BNC) cables to identify defects along the cable. The electrical configuration of BNC cables consists of a copper wire and an insulation barrier. The latter is placed at a constant distance from the copper wire, and the resistance per unit length is constant and equals to 50 Ohms. This study offers to adopt the idea of the BNC configuration by using embedded continuous carbon rovings to locate damage along TRC elements. Damage in this study defines as cracks. Two parallel carbon rovings are connected to a designated data acquisition (DAQ) system, one roving functions as the signal and the other as the insulation.

The carbon rovings have a unique micro-structure, which is divided into two zones: the inner (core) filaments and external (sleeve) filaments [8,11,15]. The sleeve filaments break due to cracking, which yields changes in the electrical current density

distribution along the roving. This phenomenon results in an increase of the impedance. In addition, the impedance is not a constant value along the carbon roving and depends on the length of the roving. These properties may limit a direct implementation of the BNC concept which will be reflected by the monitoring capabilities.

To isolate the influence of the electrical properties of the cement body, the study uses magnesium phosphate cement (MPC) matrix. MPC is a production of acid-based solution, dead burnt magnesia, potassium-based phosphate and ammonium-based phosphate [4]. MPC matrix is characterized by a relatively high impedance value compared to conventional cement-based matrix [4]. As a result, it is a better choice to reduce external environmental emissions.

To demonstrate the proposed sensory concept, the study experimentally investigates two textile reinforced MPC elements under uniaxial tensile loading tests and presents the potentials of the proposed monitoring system.

## MATERIALS AND METHOD

This study uses a generic production process of textile reinforced cement elements [4-7,12,17]. The mechanical and electrical properties of the textile and the production process of the textile reinforced MPC specimens are discussed in this section.

### Carbon-based textile

Following [4-7,12,17], the current study uses a generic textile mesh. The textile consists of six carbon rovings in the longitudinal direction ( $0^\circ$ ) and AR-glass rovings in the transverse direction ( $90^\circ$ ). The textile has a warp-knitted grid structure with a mesh size of 7-8 mm. The stitch type is pillar. The mechanical and electrical properties of the carbon and the AR-glass rovings are given in Table 1.

**Table 1.** Material properties of the AR-glass and the carbon rovings [5].

	AR-Glass roving	Carbon roving
Specific mass density [kg/m <sup>3</sup> ]	2,680	1,810
Modulus of elasticity [GPa]	72	270
Filament Tensile strength [MPa]	1,700	5,000
Filament diameter	19 $\mu$ m	7 $\mu$ m
Linear Density [tex]	2,400	1,600
Electrical resistance [ $\Omega$ /m]	Infinity	13

### MPC matrix with additive short aramid fibers

The study uses a commercial matrix of mono-potassium phosphate acid produced by ICL Group Ltd. Its commercial name is Phosment. In addition, to improve the ductility of the matrix short aramid fibers (AF) were added to the mixture. The volume fraction of the fibers is determined as 0.5%. The study uses a commercial AF named Technora CF32 produced by Teijin Frontier company Ltd. The short AF are 3mm length 12 filaments: 12  $\mu$ m diameter, the tenacity - 2.3-2.5 N/tex, mass density - 1.39 g/cm<sup>3</sup>, tensile strength - 3.2-3.5 GPa, modulus of elasticity - 65-85 GPa, elongation break - 3.9-4.5%. The MPC matrix was prepared with a ratio of 1:4 water to dry material.

The tensile and flexural strengths of the matrix (MPC +0.5% short AF) specimens were determined at 14 days according to EN 196-1:2005 [3]. The tensile and compression strengths are  $6.611 \pm 0.434$  MPa and  $61.929 \pm 6.172$  MPa, respectively.

### Carbon-based textile reinforced MPC beams

Two beams are investigated. In each beam, a single textile layer is placed. The geometrical properties of both beams are 500 mm long, 50 mm wide and 8 mm thick. The textile layer is placed in the middle of the cross-section of the beams. The beams are cast in a special mold that enables to slightly pretensioned the textile upon casting, see Fig. 1.

### Loading setup

The beams are loaded under a uniaxial tensile loading with a displacement control rate 0.5 mm/min by Instron model 5966. In order to avoid local stress at the ends of the beams, aluminum panels were attached to the ends of the beams, see also [8]. A special uniaxial device was used (Instron screw side action tensile grips model 1710-116) the widths of the supports are 50 mm and they were positioned 20 mm from the beams' edges. Along the loading process, the applies load, the displacement, the impedance spectrum and the crack propagation using the digital image correlation (DIC) technique are measured (LaVision DaVis 10). The loading scheme is shown in Fig. 2.

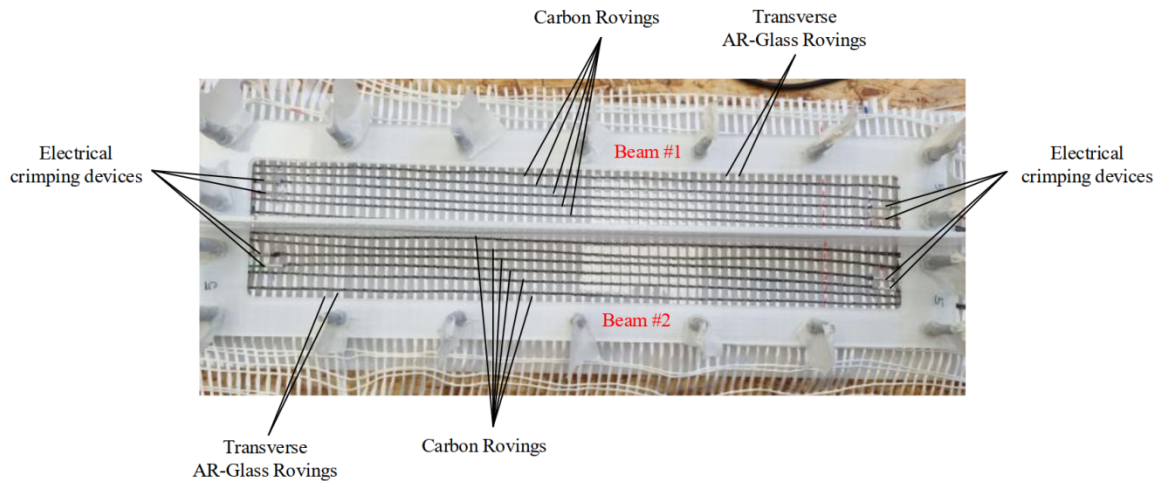


Figure 1. Casting mold for two beams.

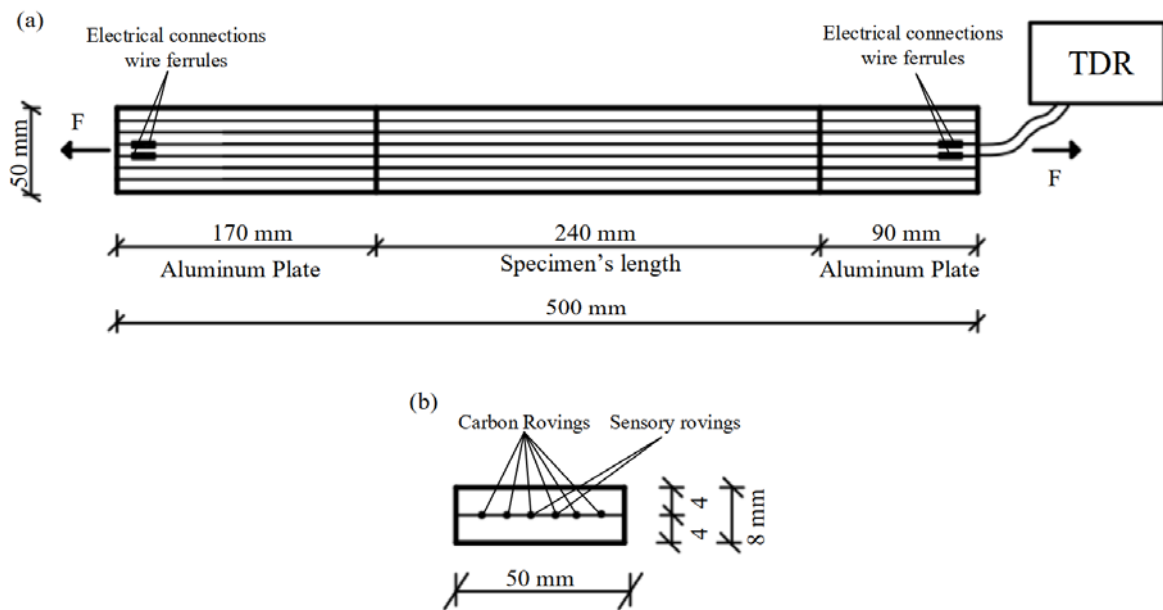


Figure 2. Experimental layout: (a) Uniaxial tensile loading beam; (b) Typical cross-section.

## SENSING CONCEPT

The study argues that by using TDR analysis, the location of damaged zones along textile reinforced MPC structures can be identified. The idea is based on sending energy pulses by an electrical current into a BNC cable. When the energy pulse encounters a damage, a portion of it is reflected. The reflection time is translated into the position of the damage. Opposed to BNC cables whose resistance per length is constant, the resistance of a carbon roving changes along the roving and depends on the structural health.

The study uses a Fieldfox Handheld Analyzer N9918B with a frequency range of 200kHz-500Mhz with 1600 reading points. Since the resistance of the carbon roving increases with the roving's length, a calibration process determines the location of the damage. The calibration is performed by a magnetic

field on a selected known zone along the element. The obtained calibrations are as follow:

$$\text{Beam A: Crack location [mm]} = 0.2231 \cdot \text{TDRindex} - 56.66 \quad (1)$$

$$\text{Beam B: Crack location [mm]} = 0.2583 \cdot \text{TDRindex} - 45.665 \quad (2)$$

The sensory process is performed by the following main three steps:

First, the measured values are determined by the following processes:

- The impedance spectrums from the TDR were measured every 1 Hz.
- The difference between every two consecutive impedance spectrums was calculated, they referred as impedance spectrum change (ISC).
- For each ISC, the peak to peak (PTP) value was calculated.

Second, the threshold values are estimated by the following process:

- The first 200 ISC were evaluated at an unloaded position and aim to estimate the noise level. The noise level evaluated by the maximum PTP of the readings (for each ISC). In our case the noise level for beam A and beam B are 0.016  $\Omega$  and 0.011  $\Omega$ , respectively.
- After the loading started, each PTP value higher than 30% of the noise level, is eligible for further investigation and considered as potential damage events.

Third, the identification of damage events is performed by:

- At the potential events the maximum PTP was investigated. Since the formation of cracks yields an integrative increase of the ISC [4,5], it is assumed that the occurrence of damage events should yield a local maximum in the ISC. In such a case, the index of the maximum PTP determines the damaged zone by the calibration presented in Eqs. [1] and [2].

## RESULTS AND DISCUSSION

Results of the experimental investigation are given in Figs. 3-6. The impedance response spectrum is measured in a frequency range of 200kHz-500MHz, with 1600 points, in a rate of 1 Hz. Fig. 3a and Fig. 5a present the load-deflection curve, the dashed vertical lines represent the formation of cracks. Cracks are considered as damage and their formation are called event #. Fig. 3b and Fig. 5b present the propagation of the cracks (measured by the DIC technique) versus the vertical deflection of beams A and B, respectively. Fig. 3c and Fig. 5c present the peak-to-peak values of the ISC for beams A and B, respectively. Therefore, the figures present the first and second main steps of the identification procedure. Fig. 4 and Fig. 6 represent a comparison between the identified position of damage by using the TDR analysis (the third step) and the actual position by using the DIC technique for beams A and B, respectively.

From the structural point of view, Fig. 3a and Fig. 5a, it is seen that both beams have similar structural responses. Beam A and beam B have four and three events, respectively. Each event represents a formation of a micro crack. The objective of the monitoring system is to identify these events.

From Fig 3c and Fig. 5c, it is seen that in both beams all the damage events are successfully identified. It is seen that in case of beam A, along

with the actual events an additional event was identified, marked in a red circle in the Fig. 3c.

According to the third step for each potential event the PTP profile and its peak was investigated. The position of the damaged zone is calculated by the obtained index and transformed to physical location by the calibration formulas. From Fig. 4a and 6a it is observed that in both beams the first damage zone is successfully identified. Yet, the locations of the next damaged zones were failed to be detected. These results are associated to the degradation of energy pulse along the carbon roving due to two main reasons: first, loss of the energy pulse after an encounter of the previous damage. In our case, a portion of the energy pulse as the first damage occurred; second, since in carbon rovings, the impedance changes along the roving, the ability to distinguish and locate damage zones that are located relatively far from the energy source reduces.

These observations demonstrate the potential of using TDR analysis to locate damaged zones in reinforced MPC structures. Yet, advanced investigation is needed to yield a robust monitoring system.

## CONCLUSIONS

The paper presented a preliminary demonstration of using TDR technique to locate cracked zones in TRC structures. The goal was to explore the ability of the technique to identify the damaged zones in TRC beams. Two specimens were loaded under uniaxial tensile loading and were monitored along the loading process. It was demonstrated that TDR technique can successfully identify the occurrence of all damage events. The first damaged zones were also successfully identified, while the exact location of the next damaged zones could not be identified. The reasons are associated to the loose of energy signal and the distance from the energy source. Despite of that, this investigation demonstrated the potential of using of TDR analysis for structural health monitoring applications. These preliminary results open the way for the development of advanced investigations that will further bring the concept of selfsensory carbon roving into realization.

**Acknowledgements:** *This research was supported by the ISRAEL SCIENCE FOUNDATION (grant No. 1663/21). The authors are thankful for the help of Eng. Barak Ofir and of the technical and administrative staff of the National Building Research Institute at the Technion. The authors acknowledge the support provided by ICL Group Ltd for providing the MPC mixture (Phosment) and by Teijin Frontier company Ltd for providing the short aramid fibers.*

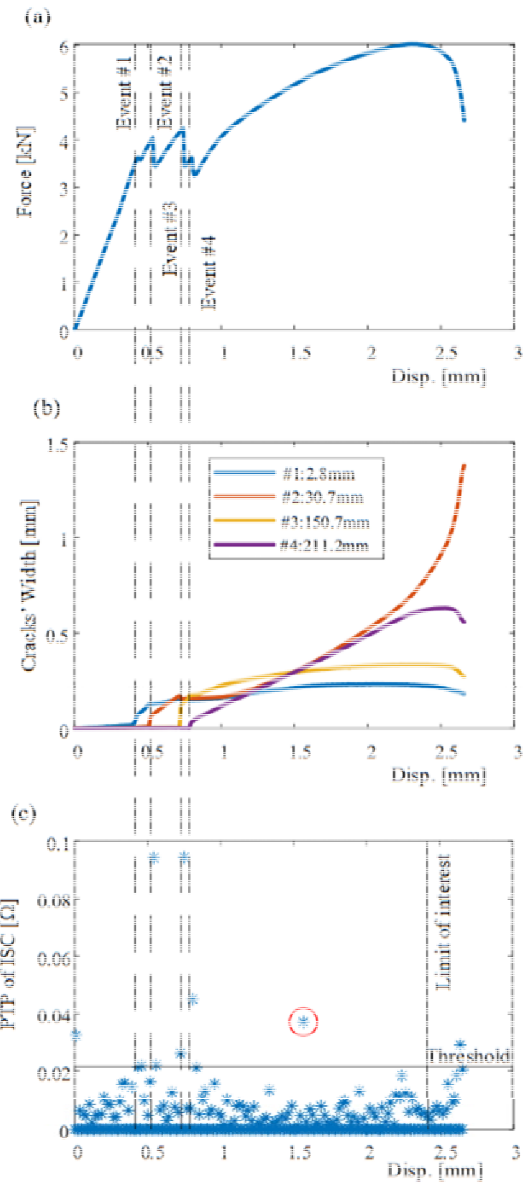


Figure 3. Mechanical and TDR analysis of Beam A: (a) Load- deflection curve; (b) PTP of ISC; (c) Cracks' propagation.

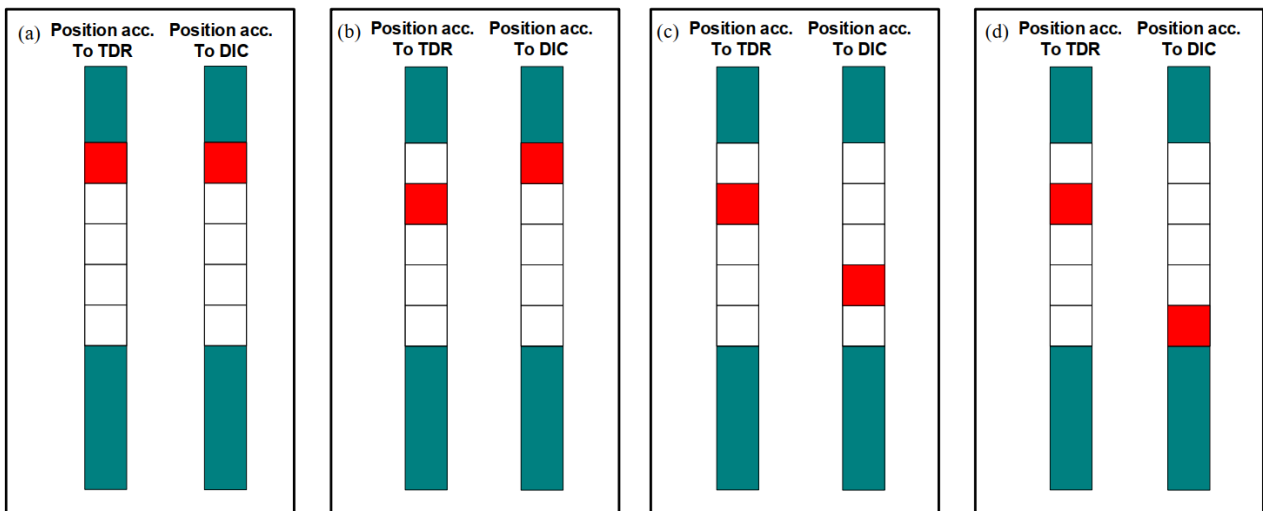


Figure 4. Position of damage comparison between the proposed method and the actual damage by DIC results for Beam A: (a) Event #1; (b) Event #2; (c) Event #3; (d) Event #4.

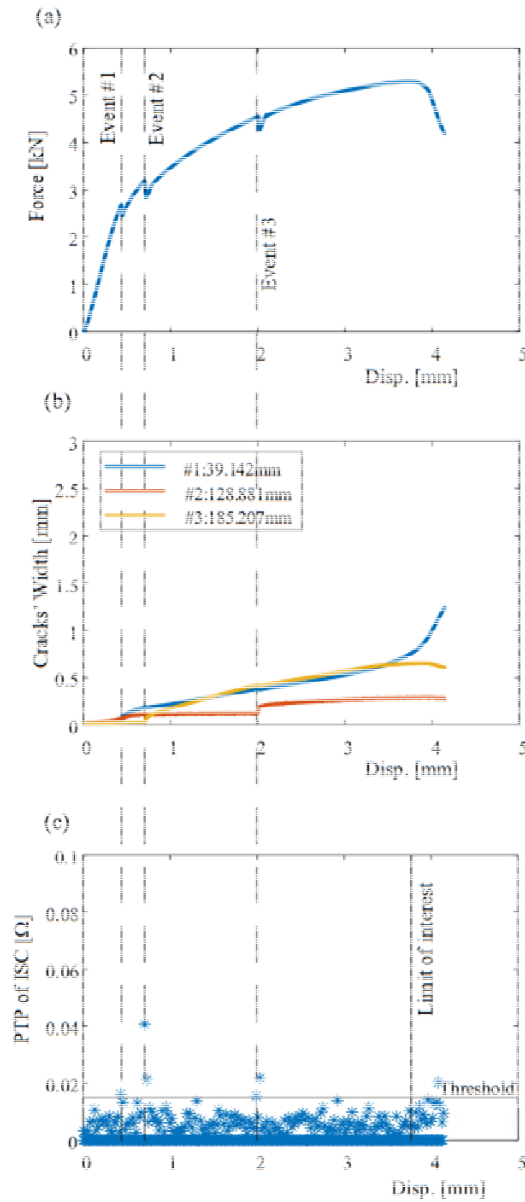


Figure 5. Mechanical and TDR analysis of Beam B: (a) Load- deflection curve (b) PTP of ISC; (c) Cracks' propagation.

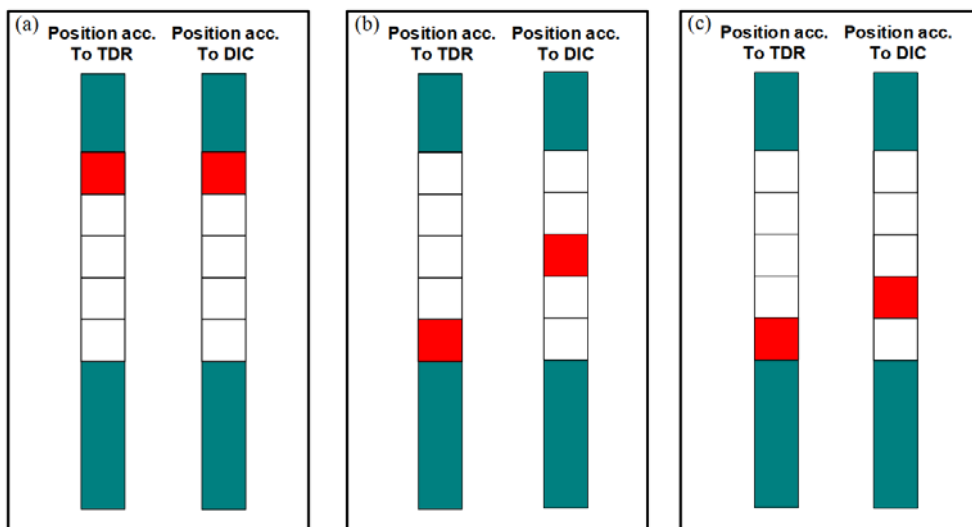


Figure 6. Position of damage comparison between the proposed method and the actual damage by DIC results for Beam B: (a) Event #1; (b) Event #2; (c) Event #3.

## REFERENCES

1. Christner, C., Horoschenkoff, A., Rapp, H., (2012). Longitudinal and transvers strain sensitivity of embedded carbon fiber sensors, *Journal of Composite Materials*. 47 (2), 155-167  
<https://doi.org/10.1177/0021998312437983>
2. De Andrade Silva, F., Butler, M., Mechtcherine, V., Zhu, D., Mobasher, B., (2011). Strain rate effect on the tensile behavior of textile-reinforced concrete under static and dynamic loading. *Materials Science and Engineering: A*, 528(3), 1727-1734.  
<http://dx.doi.org/10.1016/j.msea.2010.11.014>
3. En, B. S., (2005). 196-1. (2005). *Methods of testing cement. Determination of strength*. British Standards Institute.
4. Gaben, M., Goldfeld, Y., (2022). Enhanced self-sensory measurements for smart carbon-based textile reinforced cement structures. submitted for publication.  
<https://doi.org/10.1016/j.measurement.2023.112546>
5. Gaben, M., Goldfeld, Y., (2022). Self-sensory carbon-based textile reinforced concrete beams– Characterization of the structural-electrical response by AC measurements. *Sensors and actuators A: Physical*, 334, 113322.  
<https://doi.org/10.1016/j.sna.2021.113322>
6. Goldfeld, Y., Perry, G., (2018). Electrical characterization of smart sensory system using carbon based textile reinforced concrete for leakage detection. *Materials and Structures*, 51(6), 170.  
<http://dx.doi.org/10.1617/s11527-018-1296-7>
7. Goldfeld, Y., Yosef, L., (2019). Sensing accumulated cracking with smart coated and uncoated carbon based TRC, *Measurement*. 141, 137-151.  
<https://doi.org/10.1016/j.measurement.2019.04.033>
8. Häußler-Combe, U., Hartig, J., (2007). Bond and failure mechanisms of textile reinforced concrete (TRC) under uniaxial tensile loading. *Cement and Concrete Composites*, 29(4), 279-289.  
<https://doi.org/10.1016/j.cemconcomp.2006.12.012>
9. Hegger, J., Voss, S., (2008). Investigations on the bearing behavior and application potential of textile reinforced concrete. *Engineering Structures*, 30, 2050-205.  
<https://doi.org/10.1016/J.ENGSTRUCT.2008.01.006>
10. Peled, A., Bentur, A. (2003). Fabric structure and its reinforcing efficiency in textile reinforced cement composites. *Composites Part A: Applied Science and Manufacturing*, 34(2), 107-118.  
[https://doi.org/10.1016/S1359-835X\(03\)00003-4](https://doi.org/10.1016/S1359-835X(03)00003-4)
11. Perry, G., Dittel, G., Gries, T., Goldfeld, Y., (2021). Monitoring capabilities of various smart self sensory carbon-based textiles to detect water infiltration. *Journal of Intelligent Material Systems and Structures*, 1045389X211006901.  
<https://doi.org/10.1177/1045389X211006901>
12. Quadflieg, T., Stolyarov, O., Gries, T., (2016). Carbon rovings as strain sensors for structural health monitoring of engineering materials and structures. *Journal of strain analysis for engineering design*, 51(7), 482-492.  
<https://doi.org/10.1177/0309324716655058>
13. Shames, A., Horstmann, M., Hegger, J., (2014). Experimental investigations on Textile-Reinforced Concrete (TRC) sandwich sections. *Composite Structures*, 118, 643-653.  
<http://dx.doi.org/10.1016/j.compstruct.2014.07.056>
14. Soranakom, C., Mobasher, B., (2009). Geometrical and mechanical aspects of fabric bonding and pullout in cement composites. *Materials and structures*, 42(6), 765-777.  
<http://dx.doi.org/10.1617/s11527-008-9422-6>
15. Wen, S., Wang, S., Chung, D. D. L., (1999). Carbon fiber structural composites as thermistors. *Sensors and Actuators A: Physical*, 78(2-3), 180-188.  
[https://doi.org/10.1016/S0924-4247\(99\)00240-X](https://doi.org/10.1016/S0924-4247(99)00240-X)
16. Yosef, L., Goldfeld, Y., (2020). Smart self-sensory carbon-based textile reinforced concrete structures for structural health monitoring. *Structural Health Monitoring*, 1475921720951122.  
<https://doi.org/10.1177/1475921720951122>